Journal of Physics:
Conference Series

PURPOSE-LED
PUBLISHING™

PAPER • **OPEN ACCESS**

On the Impact of Surface Thermal Conditions on Aero-heating to Hypersonic Vehicle

To cite this article: Ahmed Yassin *et al* 2025 *J. Phys.: Conf. Ser.* **3070** 012006

View the article online for updates and enhancements.

This content was downloaded by mohamed.mab from IP address 154.186.120.120 on 07/08/2025 at 07:26

Journal of Physics: Conference Series **3070** (2025) 012006 doi:10.1088/1742-6596/3070/1/012006

On the Impact of Surface Thermal Conditions on Aero-heating to Hypersonic Vehicle

Ahmed Yassin[1], M. Ahmed[1*], Osama K. Mahmoud [1]

[1] *Aerospace Engineering Department, Military Technical College, Cairo, 11776, Egypt*

[*]E-mail: Mahmoud.yehia@mtc.edu.eg

Abstract. A numerical simulation tool is utilized to predict the heat flux distribution on the surface of a hypersonic vehicle flying at Mach 10. The study considers multiple factors influencing heat flux distribution, such as variations in isothermal wall temperature and nose radius. Additionally, it examines the adiabatic and adiabatic-radiation wall temperatures along the body surface. The model incorporates thermal non-equilibrium real gas properties and accounts for vibrational and electronic energy modes. Air is modeled as a mixture of five non-reacting species, with dynamic viscosity, specific heat, and thermal conductivity determined using non-equilibrium kinetic theory. This approach ensures accurate representation of the transport properties of gases in non-equilibrium states. The computational results are accurately validated against published experimental data to ensure the accuracy and reliability of the predictions.

1. Introduction

For decades, hypersonic aerodynamics has been a common topic for military and non-civilian applications including ballistic missiles and space vehicles. Recently however, studying hypersonic aerodynamics is proven crucial for advancing civil aviation, promising faster, more efficient, and environmentally-friendly air transportation. This development demands significant advancements across various disciplines, rendering it a challenging yet exciting area of research for the aviation industry. Possibilities of hypersonic passenger transport are explored in many endeavors yet still in conceptual or early stages of development. Advancing examples include Stargazer [1], Hexafly [2], and Destinus [3].

Content from this work may be used under the terms of the Creative Commons Attribution 4.0 licence. Any further distribution of this work must maintain attribution to the author(s) and the title of the work, journal citation and DOI.
Published under licence by IOP Publishing Ltd

The field of hypersonic aerodynamics examines the complexities of airflow, heat transfer, and structural integrity at speeds where shockwaves, elevated temperatures, and rarified air play crucial roles. In contrast to subsonic and supersonic flight, where aerodynamic phenomena are more easily anticipated and managed, the hypersonic regime presents a countless of new considerations and engineering challenges. Hypersonic aero-heating analysis is a critical aspect of studying the thermal challenges associated with vehicles, which propel through atmosphere; the intense aerodynamic interaction generates substantial heat due to compression and friction with the air molecules. The analysis involves a comprehensive examination of the thermal loads experienced by the vehicle surface, requiring an understanding of complex phenomena such as shock boundary layer, viscous-inviscid interactions, boundary layer heating, and material response to extreme temperatures.

Heat transfer to a hypersonic vehicle is a complex phenomenon that involves multiple factors including surface curvature, surface emissivity, wall thermal conditions, flight conditions (speed and angle of attack), and air composition. A smaller surface curvature radius can lead to a higher local heat flux due to the increased velocity gradient near the stagnation point.

In contrast, a higher surface temperature can lead to decreased heat transfer due to the reduction in temperature difference between the vehicle surface and the surrounding air. Adiabatic wall condition occurs when the outer wall temperature, exposed to a fluid flow, reaches the same temperature of the adjacent flow such that heat exchange between the surface and the surrounding fluid ceases. At this condition, the wall temperature reaches a maximum value. Practically, this can be attained if the wall is exposed to aero-heating for a long period of time. The highest value of adiabatic wall takes place if no radiation from the wall back to air occurs. This is expressed as the wall having no emissivity.

Adiabatic wall value decreases if the wall has finite emissivity; such value is referred to as the adiabatic radiation wall temperature. Adiabatic-radiation wall temperature refers to the temperature of a wall exposed to a fluid flow when both adiabatic and radiative heat transfer processes are considered. In this scenario, the surface neither gains nor loses heat to the surrounding fluid due to adiabatic conditions, while radiation exchanges occur between the surface and its environment.

Whether the surface acquires adiabatic (equilibrium) or radiation adiabatic conditions defines the level of heat transfer. It is as well confirmed that heat flux relates linearly to wall temperature in perfect gas flow and to wall enthalpy in chemical non-equilibrium flow. However, under radiation equilibrium conditions, heat flux varies notably due to spatial variation in wall temperature. Similarly, high surface emissivity can effectively radiate heat away from the vehicle, consequently reducing the aggregate heat flux. A higher Mach number can lead to increased heat transfer while the angle of attack can significantly affect the heat transfer distribution on the vehicle. Finally, air composition can alter heat transfer, with air containing a higher concentration of oxygen leading to increased heat transfer due to the increased chemical reaction rates.

In hypersonic flow, the effect of wall temperature on the vibrational energy of molecules is significant and complex. Elevated wall temperatures lead to increased kinetic energy of molecules near the wall, which in turn results in higher vibrational energy. This phenomenon occurs due to the intense thermal environment characteristic of hypersonic flow, where molecules experience rapid collisions and interactions with the hot wall surface.

The increased wall temperature promotes greater molecular motion and collision frequencies, causing molecules to absorb more energy and exhibit higher vibrational states. Additionally, higher temperatures can induce dissociation and ionization of molecules near the wall, further contributing to elevated vibrational energy levels. Conversely, lower wall temperatures in hypersonic flow environments lead to reduced vibrational energy as molecules possess less kinetic energy and experience fewer collisions with the cooler wall surface. Overall, the effect of wall temperature on vibrational energy in hypersonic flow is a result of the intricate interplay between thermal energy transfer, molecular collisions, and chemical reactions occurring at the boundary between the flow and the solid surface.

The impact of the abovementioned factors has been the topic of researches over the years. Lee et al. [4] employed the DSMC method to compute wall heat fluxes and flowfield properties for hypersonic flows (up to Mach 25) over different leading-edge geometries, aligning closely with available experimental data. Liang et al. [5] employed Navier-Stokes equations to assess how the nose radius and corner radius affect the heating rate over a blunt body exposed to hypersonic flow at Mach number 8. Prabhu et al. [6] conducted real gas aerothermodynamic testing, uniquely allowing independent variation of velocity, effective altitude, and test gas composition. They developed a method to quantify convective heat transfer rates from high-speed thermal images of hypersonic projectiles, which aligned with real-gas Navier-Stokes computations.

Gao et al. [7] examined hypersonic flow at Mach 5 and Mach 20, around a typical blunt-headed cone. They proposed a new method using local wall enthalpy interpolation to estimate heat flux in radiation equilibrium conditions under different parameters. The used numerical approach demonstrated errors below 5%. MacManus [8] used a Parabolised Navier-Stokes (PNS) flow solver to forecast aerodynamic heating on a hypersonic vehicle surface up to Mach 8. The study explored heat flux sensitivities to various conditions for a full-scale vehicle, covering different flight phases and factors including wall temperature and turbulence level. Experimental validation showed good agreement with predictions.

Kianvashrad and Knight [9] explored how different vibrational temperature boundary conditions affect the prediction of aero-thermodynamic loading in hypersonic laminar flow at Mach 12.6 and Mach 13.2 over a hollow cylinder flare. They found that variations in these conditions at the isothermal wall had minimal impact on predicted peak surface heat transfer and surface pressure. Huang et al. [10] used a chemical non-equilibrium model to address how different air species affect heat flux. They concluded that the seven-species model produced the most accurate heat flux prediction, particularly at higher Mach numbers.

In the open literature, the scarcity of studies addressing the impact of wall thermal conditions on hypersonic aeroheating is evident. A notable gap can be highlighted regarding the role of emissivity of wall material using numerical simulation technique. Existing literature [7] implemented experimental techniques. In addition, a study on combined impact of different wall conditions is not available in the open literature. Overall, the paper aims to shed more light on this increasingly-important topic of hypersonic flight with focus on impact of wall thermal conditions on aero-heating.

2. Case-study and Methodology

2.1 Case study

The case study represents the forebody of a typical hypersonic vehicle. It has a hemispherical cap followed by a cone, a tangent ogive, then another cone with total slenderness ratio of 3.41 (referred to base diameter), Figure 1. The cap has a bluntness ratio of 0.04. The first cone section has a semi-apex angle of 18 degrees and slenderness ratio of 0.0018. The subsequent tangent-ogive section has a slenderness ratio of 0.5. The final cone section has a fineness ratio of 2.8 and semi-apex angle of 7 degrees. The vehicle is flying at Mach 10 and zero incidence at altitude of 60 km with air pressure and temperature of 20.314 Pa and 245.45 K, respectively.

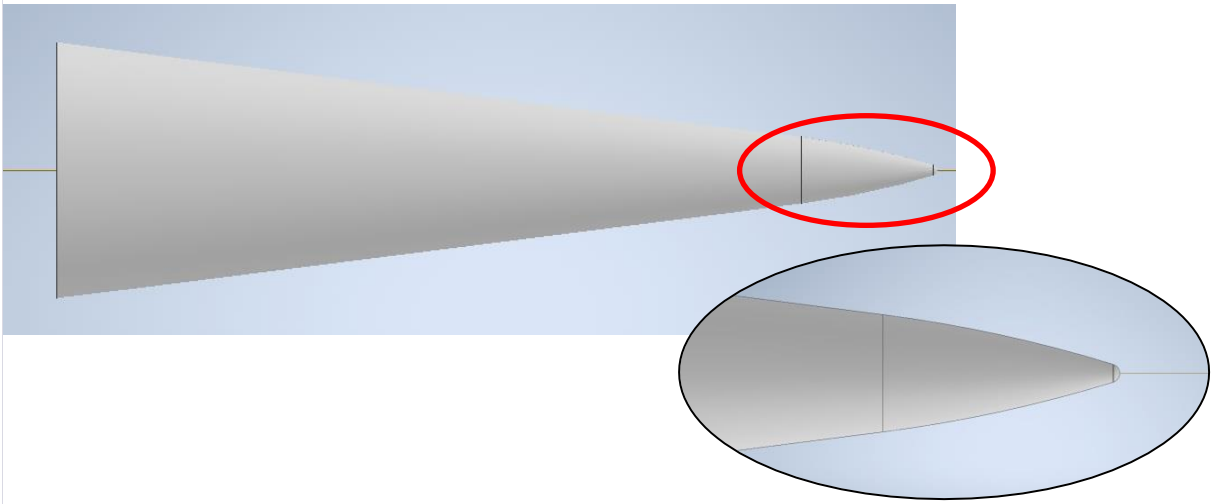

Figure 1. Geometry of the case study hypersonic vehicle.

2.2 Setup of Numerical simulations

The objective of the study is to explore the impact of wall thermal conditions on aeroheating. A set of numerical simulation cases are designed to achieve the goals of the present study. Table 1 provides an overview of setup of the eight cases in concern. For all cases, freestream conditions remain consistent featuring flight at the altitude of 60 km with Mach 10.

Table 1. Setup of computational analysis cases

Case No.	Wall condition		Nose bluntness	Emissivity Coefficient ε	Objective
1	Isothermal, [K]	300	0.04	n/a	Impact of nose bluntness
2			0.03		
3			0.02		
4		500			Impact of wall temperature
5		700			
6	Adiabatic				Impact of adiabatic wall condition and emissivity
7	Adiabatic-Radiation			0.8	
8	Adiabatic-Radiation			0.9	

The first case, serving as the baseline for comparison, is the primary case. Subsequent cases involve variations in wall conditions. The second and third cases correspond to configurations with variable nose bluntness. The fourth and fifth cases pertain to scenarios with isothermal walls at different isothermal temperatures. The sixth case illustrates the scenario with adiabatic wall condition assuming no radiation while the seventh and eighth cases depict instances with adiabatic radiation walls featuring emissivity coefficients 0.8 and 0.9.

As the angle of attack is zero, all simulations are conducted in a 2D axisymmetric plane shown in figure 2. At the inlet, freestream conditions are defined while at exit boundary, total temperature is defined. The body boundary is defined as a non-slip wall with thermal conditions varying from one case to the other according to the table above. The domain is discretized with a first cell height at the walls of 7.5×10-8 meters. This fine resolution yields a local cell Reynolds number Rec at the stagnation point of 0.00123, which is well below 1. The domain is comprised of about 247,000 cells.

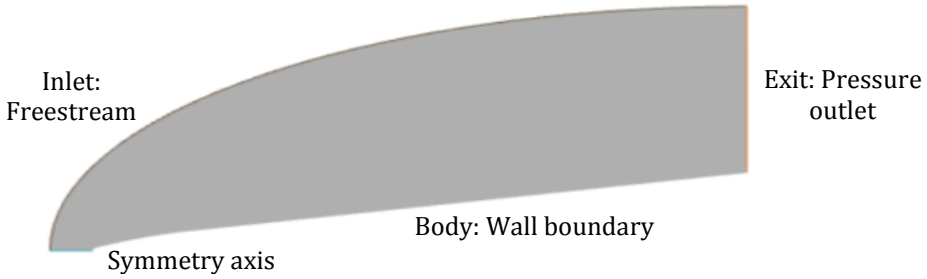

Figure 2. The computational domain

A commercial CFD solver [11] is implemented in the present study. Numerical simulations are conducted utilizing the AUSM+ flux vector splitting inviscid flux scheme for its superior suitability in addressing hypersonic flows. Additionally, a 3rd order convection scheme, MUSCL, is employed to enhance accuracy, particularly in capturing intricate phenomena such as shock waves, wakes, vortices, and discontinuities, by reducing numerical dissipation. Time integration is accomplished through a backward Euler implicit non-iterative scheme. The size of each time step is determined based on stability criteria, particularly the CFL number.

The selection of the Equation of State Model is based on the Thermal Non-Equilibrium Real Gas model, available in the CFD solver and specifically tailored for applications in conditions characterized by high temperatures and low densities. In such scenarios, the vibrational/electronic energy modes become effective, while the density remains low enough to prevent equilibration [12]. To simplify the simulation, a multi-component, non-reacting model is assumed implying no exchange reactions between the molecules.

Air composition consists of five species with the following molecular ratios: N_2 (0.74), O_2 (0.22), N (1.0×10^{-5}), O (0.001), and NO (0.03899). Flow parameters are computed individually for each gas component in the system. Dynamic viscosity is determined using Chapman-Enskog theory, which describes the behavior of gases under non-equilibrium conditions. Specific heat is calculated assuming all vibrational modes are fully excited. Thermal conductivity is determined using non-equilibrium kinetic theory, which accounts for the transport properties of gases in non-equilibrium states. These methods allow for accurate characterization of the fluid properties in diverse gas mixtures and conditions.

3. Results and Discussions

3.1 Validation of CFD model

Holden et al. [13] conducted an experimental study in a shock tunnel to measure heat transfer and pressure in shock/shock interaction regions within laminar, low-density flows at Mach numbers 11 to 16 and Reynolds numbers 800 to 8,000. They used cylindrical leading edges with nose radii of 3.5 mm, 9.5 mm, and 38.1 mm, each equipped with high-resolution thin-film heat transfer instrumentation. One case from the series of test conditions was chosen as a reference case for a detailed validation study. This case will be used to evaluate the model precision in predicting heat flux distributions along the surface of the cylindrical leading edge. Table 2 offers a comprehensive overview of the flight boundary conditions applied during the selected experimental test. It also details the dimensions of the cylindrical leading edge used in the study.

Table 2. Boundary conditions applied during the experimental test

Mach No	Pressure [Pa]	Temperature [K]	Reynolds Number [1/m]	(Isothermal) Wall Temperature [K]	Cylinder Diameter [m]	Flow Speed [m/s]
16.01	21.8357	43.216667	1187007.87	300.33	0.0381	2111

Figure 3 compares the measured and calculated values of local heat flux distribution over the hemispherical body. The figure demonstrates that the heat flux calculated using the specified CFD model aligns well with the experimental data [13] confirming the model accuracy and reliability in predicting heat flux at hypersonic speeds. The model can be further validated by comparing the computed value of peak heat flux at the stagnation point to those measured by Holden [13] and predicted by Fay and Riddell [14]. The comparison is held in Table 3.

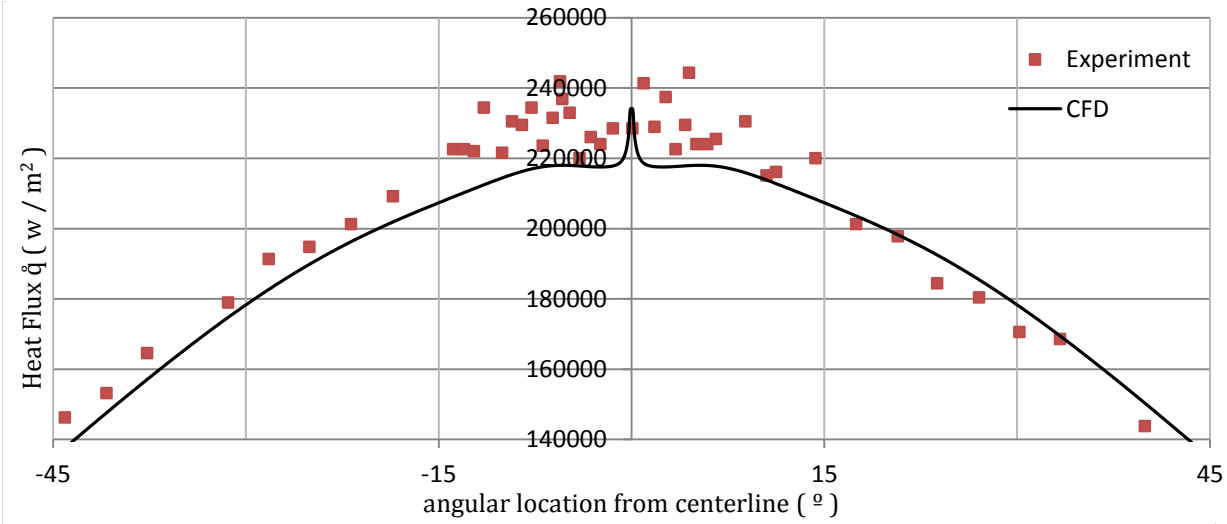

Figure 3. Comparison between the computed and measured values of heat flux distribution

Table 3. Comparison of numerical, experimental, and theoretical values of peak heat flux at the stagnation point

	Value [watt]			% Deviation of CFD value	
	Experiment [12]	Theory[13]	CFD	from experiment	from theory
Peak heat flux	228419.06	207143.26	233936.6	2.14	12.93

3.2 Results of the case study simulations

3.2.1 The Effect of Nose Radius

The impact of nose radius on aeroheating is addressed by comparing the findings of cases 1 to 3, Table 1, representing nose bluntness of 0.04, 0.03 and 0.02. Table 4 outlines the contrast in heat transfer to the entire body and heat flux at the stagnation point for the three different cases assuming isothermal wall conditions. Values based on Fay-Riddell's theory [14] are listed as well for the sake of comparison. Deviation of simulation results is below 9%.

Nose radius has a significant impact on heat flux to the stagnation zone. For instance, as the nose radius is reduced to half, heat flux is increased by more than 40%. However, the total heat transfer to the entire body is not as sensitive to nose bluntness.

Table 4. Impact of nose bluntness on heat flux to the case study vehicle

Nose bluntness		0.04	0.03	0.02
Total heat transfer rate to the whole body [w]	CFD	110389	126242	139251
Peak heat flux at the stagnation point [w/m2]	CFD	590350	707628	845707
	Theory [14]	647370	747519	915520
	% deviation	8.8	5.34	7.64

3.2.2 The Effect of Wall Temperature

To assess how wall temperature impacts aeroheating characteristics, three cases namely, 1, 4, and 5 are compared representing isothermal wall temperatures of 300K, 500K and 700K, respectively. Table 5 displays the heat transfer to the whole vehicle and heat flux at the stagnation point at different isothermal wall temperatures. For the sake of validation, the corresponding theoretical values of stagnation heat flux based on Fay-Riddell's theory [14] are also listed. The deviation is below 9%. Typically, heat transfer to the vehicle decreases as the isothermal temperature increases. At the extreme case, heat transfer ceases as the wall temperature approaches the adiabatic wall value.

Table 5. Impact of isothermal wall temperature on heat flux to the case study vehicle

Isothermal wall temperature, K		300	500	700
Total heat transfer rate to the whole body [w]	CFD	110389	104093	94840
Peak heat flux at the stagnation point [w/m2]	CFD	590350	564609	529363
	Theory [14]	647370	615709	584474
	% deviation	8.8	8.3	9.4

Generally, the wall temperature has a slight impact on heat transfer. Increasing wall temperature from 300 to 700 K (2.5 times higher) yields only 10% drop in heat transfer. Nonetheless, heat transfer to the vehicle is not uniform. Figure 4 illustrates the heat flux distribution along the body at wall temperature of 700 K. heat transfer is maximum at the stagnation region and drops rapidly downstream until it reaches about 3% of its stagnation value.

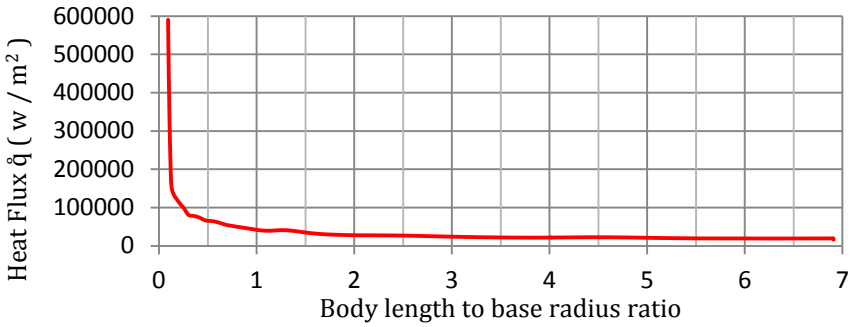

Figure 4. Heat flux distribution along the body at isothermal wall temperature of 700 K

3.2.3 The Condition of Adiabatic Wall Temperature:

The role of adiabatic and radiation adiabatic wall conditions at different and emissivity values is explained by contrasting cases 6, 7, and 8, Table 1. Table 6 presents the calculated peak adiabatic wall temperature values at the stagnation point for three different wall emissivity conditions.

Table 6. Peak adiabatic wall temperature values for three different wall emissivity conditions

Wall condition	adiabatic (no emissivity)	radiation adiabatic (ε = 0.8)	radiation adiabatic (ε = 0.9)
Adiabatic Wall Temperature [K]	4297	1505	1429

The adiabatic wall temperature at stagnation point decreases by approximately 65 to 66.7% from its recovery value when using materials with emissivity coefficients of ε = 0.8 and 0.9, respectively. This highlights the significance of selecting high-emissivity materials in structural design. At such high values of emissivity, increasing emissivity has a minor impact on wall temperature. Figure 5 displays the distribution of adiabatic wall temperature along the body. Initially, the stagnation point exhibits the highest wall temperature. Subsequently, there is a noticeable decrease in the temperature along the vehicle body until it reaches approximately 46% of stagnation point value at the base of the vehicle.

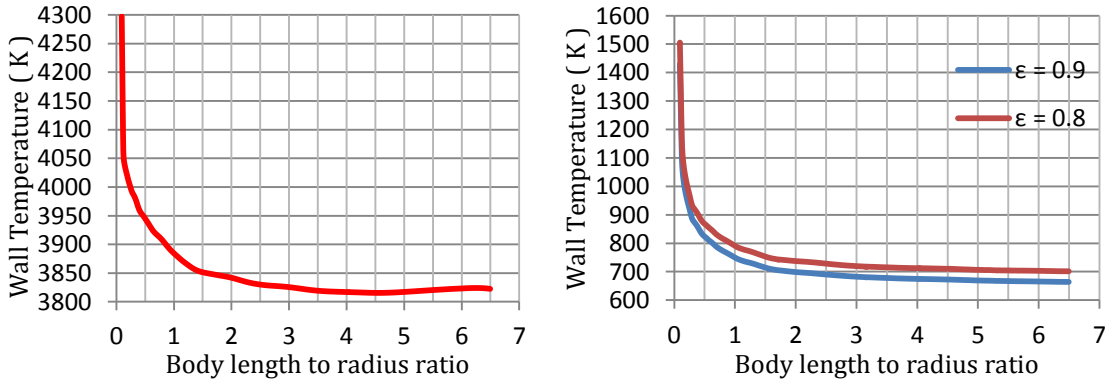

(a) adiabatic wall (b) radiation-adiabatic wall

Figure 5. Comparison between adiabatic wall temperature values for three different wall emissivity conditions

4. Conclusion

The field of hypersonic aerodynamics has gained recent interest from researchers by virtue of emerging civil applications. One defining feature of hypersonics is the aero-heating to the vehicle wall. In this respect, the thermal conditions of the wall have decisive role. The present paper sheds more light on the impact of wall conditions on aero-heating to a typical hypersonic vehicle at Mach 10. A commercial numerical simulation tool is utilized. The model accounts for thermal non-equilibrium real gas properties along with vibrational/electronic energy modes. Air is assumed as composed of five non-reacting species and dynamic viscosity, specific heat, and thermal conductivity are determined using non-equilibrium kinetic theory, which accounts for the transport properties of gases in non-equilibrium states. The simulation model is validated against published experimental data.

The study confirmed the significant impact of emissivity on the level of thermal loads on the wall. It also confirmed the slight impact of emissivity value and wall temperature on heat flux. Impacts of surface curvature and wall temperature are also addressed.

The study is sought to be extended to explore the aeroheating to a complete hypersonic vehicle. The impact of flow features and aeroheating on vehicle air-breating propulsion elements will be addressed.

5. References

[1] https://www.venusaero.com/meet-stargazer-the-new-hypersonic-plane-that-will-fly-from-new-york-to-tokyo-in-one-hour/

[2] G. Pezzella, M. Marini, M. Cicala, A. Vitale, T. Langener and J. Steelant, 'Aerodynamic Characterization of HEXAFLY Scramjet Propelled Hypersonic Vehicle', 32nd AIAA Applied Aerodynamics Conference, AIAA2014-2844, Aviation 2014, 16-20 June 2014, Georgia, Atlanta, USA.

[3] Jimmy-John O.E. Hoste, Dominique Charbonnier, Andrés Zarabozo, Ambara Bernabeu-Vazquez and Tomasz Witkowski., “An overview on the use of CFD in the development of hypersonic vehicles at Destinus” 2nd International Conference on High-Speed Vehicle Science & Technology 11–15 September 2022, Bruges, Belgium.

[4] Jiang Y, Gao Z, Jiang C, Lee C-H. Hypersonic aeroheating characteristics of leading edges with different nose radii. J Thermophys Heat Transf 2017; 31(3): 538–48.

[5] Liang, Z., Zhi, C., Jian, G. and Xuejun, Z., 2015. Effects of Nose and Corner Radius on Heat Transfer Rates over Axisymmetric Blunt Body. Procedia Engineering, 99: pp. 428–432.

[6] Wilder, M. C., Reda, D. C., Bogdanoff, D. W., and Prabhu, D. K., “Free-Flight Measurements of Convective Heat Transfer in Hypersonic Ballistic-Range Environments,” 39th AIAA Thermophysics Conference, Miami, FL, AIAA Paper 2007-4404, 25–28 June 2007.

[7] Zepeng Yang, Suozhu Wang and Zhenxun Gao., “Studies on effects of wall temperature variation on heat transfer in hypersonic laminar boundary layer” j.ijheatmasstransfer.2022.122790.

[8] M. Mifsud, D. Estruch-Samper, D. MacManus and R. Chaplin., “A case study on the aerodynamic heating of a hypersonic vehicle” The Aeronautical Journal, SEPTEMBER 2012 VOLUME 116 NO 1183, 10.1017/S0001924000007338.

[9] Nadia Kianvashrad and Doyle Knight., “Effect of Vibrational Temperature Boundary Condition of Isothermal Wall on Hypersonic Shock Wave Laminar Boundary Layer Interaction of a Hollow Cylinder Flare” 7th European Conference for Aeronautics and Aerospace Sciences, 2017, 10.13009/EUCASS2017-97.

[10] Yipu Zhao and Haiming Huang., “Numerical study of hypersonic surface heat flux with different air species models” Acta Astronautica Volume 169, April 2020, 10.1016/j.actaastro.2020.01.002.

[11] Siemens Industries Digital Software. Simcenter STAR-CCM+, version 2022.1, Siemens 2022.

[12] lain D. Boyd., “Rotational and Vibrational Nonequilibrium Effects in Rarefied Hypersonic Flow" J. Thermophys. Heat Transfer 4,478 (1990).

[13] Holden, M.S., Kolly, J.M., and Martin, S.C., “Shock/Shock Interaction Heating in Laminar and Low-Density Hypersonic Flows”, AIAA Papers 1996-1866, June 1996.

[14] J. A. Fay and F. R. Riddell., “Theory of Stagnation Point Heat Transfer in Dissociated Air” Journal of The Aeronautical Sciences Volume 25, February 1958, Number 2, 10.2514/8.7517.